forumacusticum 2023

TOWARDS MODELING DYNAMIC HEAD-ABOVE-TORSO ORIENTATIONS IN HEAD-RELATED TRANSFER FUNCTIONS

Fabian Brinkmann[1*]   **Dannie Smith**[2]   **William J. Anderst**[3]
Sebastià V. Amengual Garí[2]   **David Lou Alon**[2]   **Stefan Weinzierl**[1]
[1] Audio Communication Group, Technische Universität Berlin, Germany
[2] Reality Labs Research at Meta, Redmond, WA, USA
[3] Department of Orthopaedic Surgery, University of Pittsburgh, PA, USA

ABSTRACT

The torso and shoulder affect the head-related transfer function (HRTF) by means of reflection and diffraction. The reflection is strongest if the ear, source, and shoulder are approximately aligned and superimposes a comb-filter upon the HRTF magnitude spectrum that can have a depth of up to 5 dB above approximately 700 Hz. In case the direct sound path to the ear is obstructed by the shoulder or torso, they act as a low-pass with a high frequency damping starting at approximately 1 kHz and reaching up to 20 dB at 20 kHz. However, relatively little is known about the exact nature of the torso effect for different head-above-torso orientations with current data being based either on simplified geometric models, a neutral head-above-torso orientation, or head-above torso rotations in a single plane. To close this gap, we aim at developing a 3D head and torso model that can rotate its head with three degrees of freedom based on a functional model of the average healthy young cervical spine. In this work, we introduce the parameterization of the model. The model can be used to numerically simulate HRTFs for the anatomically possible range of head-above-torso orientations and is intended to analyze the torso effect in more detail and to acoustically model dynamic head-above-torso movements for virtual acoustic reality.

Keywords: *head-related transfer function, head-above-torso orientation, cervical spine.*

---

*Corresponding author: *fabian.brinkmann@tu-berlin.de.*

1. INTRODUCTION

Head movements help listeners to judge spatial sound qualities, improve localization accuracy, and increase speech intelligibility in noisy environments [1–3]. They can be initiated either by the entire body during walking or turning motions or by the spine. In the latter case, independent head movements are performed by the so called cervical spine (upper part of the spine), whereas head movements in combinations with motion from the torso are performed mainly by the thoracic spine (middle part) [4]. For head movements initiated by the spine, the head-above-torso orientation (HATO) and thus the position of the ears with respect to the torso changes, which effects the amount of torso shadowing and reflection depending on the source position. Modeling head movements from the spine is therefore necessary for realistic HRTF rendering. Because the change in HATO is most pronounced for independent head movements from the cervical spine, their influence on the HRTF can expected to be more significant than the influence of combined head and torso movements from the thoracic spine. For this reason, we restrict ourselves to modelling independent head movements initiated by the cervical spine. Note that the influence of the torso is constant during head movements that are initiated from the entire body such as walking, as the HATO remains constant in these cases. Consequently, these movements do not require specific treatment for realistic HRTF rendering.

Three kinds of head movements that are physiologically fundamentally different are to be distinguished: *rotation* denotes movements in the horizontal plane, i.e., rotating the head left or right, *flexion* and *extension* denote movements in the median plane, i.e., looking up or down,

and *lateral bend* denotes movements in the frontal plane, i.e., rolling the head to the left or right [4].

Modeling head movements is a common task in computer graphics. However, such models aim at efficiently creating visually appealing head movements and lack a detailed anatomical background. More sophisticated models are used in bio-mechanics [5, 6], where they are used to predict muscle forces, internal joint forces, and forces on intervertebral discs based on motion capture or manual user input. They not designed to model in vivo kinematics, feature an arbitrary rather than a representative average skeleton and make use of simplifying assumptions. For example the OpenSim model [5] assumes a constant contribution of all vertebra to head motion and fixed centers of rotation, which is not the case as detailed in Section 2.

In the following, we describe how movements can be parameterized to obtain a dynamic head and torso model, that is, a 3D computer model that can move its head according to the average, healthy and young adult population. The following analysis discarded data from pathological samples because the head movements are potentially affected by injuries of the spine. In addition, we discarded head translations and focused on standing or upright sitting subjects as the most common and well researched case.

2. METHOD

The dynamic head above torso model consists of three building blocks that are detailed in the following. The neutral position of the cervical spine is the starting point for all head movements. The intervertebral orientation gives the rotation, flexion/extension, and bend angles of each vertebra with respect to the inferior vertebra as a function of the current head orientation. The instantaneous center of rotation (ICR) give the point about which a vertebra rotates, flexes/extends, and bends as a function of the current intervertebral orientation. The parameters for those blocks were obtained from measurements of in vivo motion and are described in the following sections.

2.1 Anatomy of the cervical spine in neutral position

The cervical spine consists of the seven vertebrae - C7 (bottom) through C1 (top), on top of which rests the Occipital bone (skull, denoted C0 in the following). Table 1 and Fig. 1 illustrate the neutral position of the cervical spine, which was determined from previously unpublished
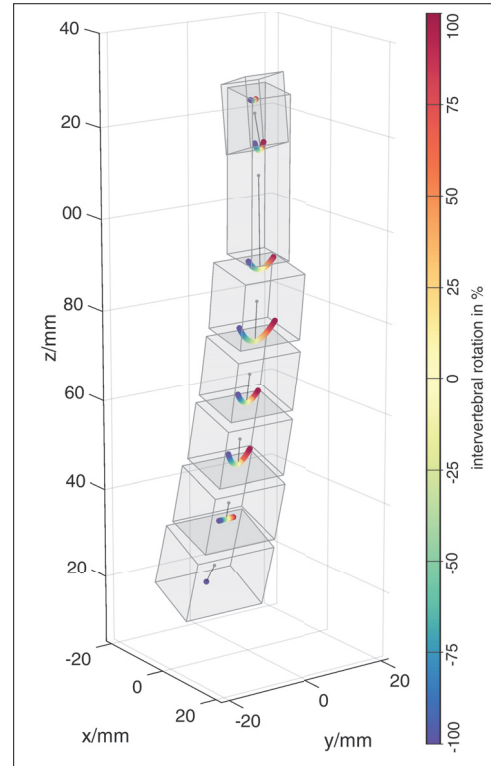

Figure 1. Schematic model of the cervical spine in neutral position (gray boxes denote the vertebral bodies) and instantaneous center of rotation paths for lateral bend (color coded). Gray lines relate the vertebra and their corresponding ICR path. The color is coded with respect to the percentage of the intervertebral motion to achieve a common color scale regardless of the intervertebral ROM. The upmost ICR path belongs to C0.

data from Anderst et al. [7] (29 subjects, 15M, 14F, average age 27.3). It is defined by the front/back displacement x and up/down displacement z of each vertebra in mm with respect to the center of the shoulders (arithmetic mean between two markers placed on the left and right acromion), the width, height, and depth of the vertebral bodies in mm, and the absolute flexion/extension angle with respect to the horizontal plane. Small left/right displacements, as well as rotation and lateral bend angles can also be observed in the neutral position but are close to zero on average and were thus neglected (cf. [8], Table 1).

Table 1. Neutral position of the average cervical spine and the upmost thoracic vertebra T1. The angle denotes flexion (negative sign) and extension (positive sign) with respect to the inferior vertebra in degree. See text for details.

	x	z	width	height	depth	angle
$C1$	2.6	124.7	8.9	9.5	14.8	12.2
$C2$	4.0	111.8	8.9	9.5	35.7	-1.7
$C3$	3.4	84.4	11.7	15.1	14.8	-9.0
$C4$	0.8	67.9	12.1	15.8	14.2	-13.0
$C5$	-2.8	52.3	12.5	16.5	13.8	-15.0
$C6$	-7.0	38.9	13.0	18.1	14.2	-17.0
$C7$	-12.5	21.0	12.9	19.9	15.6	-20.7
$T1$	-19.5	7.5	13.6	22.5	14.8	-28.1
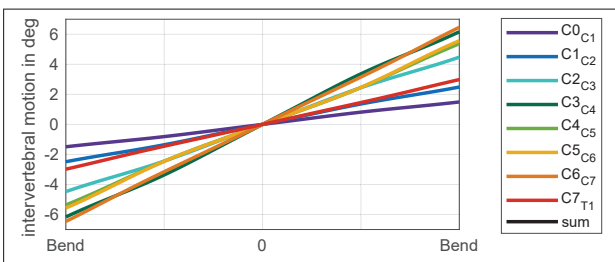
Figure 2. Intervertebral motion curves for lateral bend within the ROM of $\pm 35°$.

2.2 Intervertebral motion curves

The absolute position of the head with respect to the torso for a given head orientation depends on the current intervertebral orientation, which makes it a vital model parameter that was modeled in a two step procedure. First, the intervertebral range of (ROM), which gives the maximum possible rotation of each vertebra with respect to the inferior vertebra, was determined from published data by averaging available data using weights to account for varying sample sizes [7,9–18] (not shown here for brevity and discarding studies with an average age above 40 because the intervertebral ROM decreases with age). The absolute ROM, i.e., the maximum possible head orientation was obtained from the accumulated intervertebral ROM values and is $\pm 59.1°$ rotation ($\pm 60°$ used for the final model, achieved by scaling intervertebral ROM values accordingly), $107°$ of flexion/extension ($110°$ in the final model), and $\pm 35.1°$ lateral bend ($\pm 35°$ in the final

model). In a second step, we took existing intervertebral motion curves averaged across 29 subjects [8] (15M, 14F, average age 27.3) and given by means of fourier series coefficients of order 10. The maximum values of the curves were scaled to the desired intervertebral ROM values obtained in the first step. In case of rotation and lateral bend, the data were averaged across movements to the left and right to obtain curves that are symmetrical around the neutral position. This two step procedure was chosen to obtain a more robust estimate for the intervertebral ROM, which is well researched, to be used as a basis for the motion curves that are to our best knowledge only available from a single study. Figure 2 shows the motion curves for the example of lateral bend.

2.3 Instantaneous centers of rotation

The last parameter influencing the absolute head position is the ICR. It was measured for rotation and lateral bend by Anderst [7] (29 subjects, 15M, 14F, average age 27.3), and for flexion/extension by Anderst et al. [19] (20 subjects, 7 M, 13 F, average age 46). The data was again averaged as described above to obtain curves that are symmetrical around the neutral position. Because measurements of the ICR are prone to noise [19], the curves were smoothed by fitting polynomials to the data with orders of zero to three depending on the motion (rotation, flexion/extension, lateral bend) and vertebra. The final ICR paths are given as a function of the intervertebral orientation and the polynomial representation was used to extrapolate to missing intervertebral orientations. Fig. 1 shows the ICR paths for the example of lateral bend.

3. CONCLUSION

We introduced a functional model of the average healthy and young human cervical spine describing the neutral position of the spine as a starting point for head movements, as well as intervertebral motion curves and ICR paths to parameterize the head movements. The acquired data show that each vertebra takes a unique role within the head movement, which stresses the importance of an anatomical correct model to obtain realistic head-above-torso positions. These will later be used as a basis for assessing the acoustic effect of different HATOs by means of numerical acoustic simulations. Future studies will give a more comprehensive overview of the model parameters including data for rotation and flexion/extension as well as details on the implementation of the functional data and realization of the dynamic head and torso model.

4. REFERENCES

[1] C. Kim, R. Mason, and T. Brookes, "Head movements made by listeners in experimental and real-life listening activities," *J. Audio Eng. Soc.*, vol. 61, pp. 425–438, June 2013.

[2] K. I. McAnally and R. L. Martin, "Sound localization with head movement: implications for 3-d audio displays," *Frontiers in Neuroscience*, vol. 8, p. 210, 2014.

[3] J. A. Grange and J. F. Culling, "The benefit of head orientation to speech intelligibility in noise," *J. Acoust. Soc. Am.*, vol. 139, no. 2, pp. 703–712, 2016.

[4] D. A. Neumann, ed., *Kinesiology of the musculoskeletal system. Foundations for rehabilitation*. St. Louis, MO, USA: Elsevier, third ed., 2017.

[5] A. Seth, J. L. Hicks, T. K. Uchida, A. Habib, C. L. Dembia, J. J. Dunne, C. F. Ong, M. S. DeMers, A. Rajagopal, M. Millard, S. R. Hamner, E. M. Arnold, J. R. Yong, S. K. Lakshmikanth, M. A. Sherman, J. P. Ku, and S. L. Delp, "OpenSim: Simulating musculoskeletal dynamics and neuromuscular control to study human and animal movement," *PLOS Computational Biology*, vol. 14, p. e1006223, July 2018.

[6] J. Rasmussen, "The AnyBody Modeling System," in *DHM and Posturography* (S. Scataglini and G. Paul, eds.), pp. 85–96, Academic Press, 2019.

[7] W. J. Anderst, W. F. Donaldson, J. Y. Lee, and J. D. Kang, "Three-dimensional intervertebral kinematics in the healthy young adult cervical spine during dynamic functional loading.," *Journal of Biomechanics*, vol. 48, pp. 1286–1293, May 2015.

[8] W. J. Anderst, "Bootstrap prediction bands for cervical spine intervertebral kinematics during in vivo three-dimensional head movements," *Journal of Biomechanics*, vol. 48, pp. 1270–1276, May 2015.

[9] J. Dvorak, D. Froehlich, L. Penning, H. Baumgartner, and M. M. Panjabi, "Functional Radiographic Diagnosis of the Cervical Spine: Flexion/Extension," *Spine*, vol. 13, pp. 748–755, July 1988.

[10] M. Mimura, H. Moriya, T. Watanabe, K. Takahashi, M. Yamagata, and T. Tamaki, "Three-dimensional motion analysis of the cervical spine with special reference to the axial rotation," *Spine*, vol. 14, pp. 1135–1139, Nov. 1989.

[11] A. Holmes, C. Wang, Z. H. Han, and G. T. Dang, "The range and nature of flexion-extension motion in the cervical spine," *Spine*, vol. 19, pp. 2505–2510, Nov. 1994.

[12] W. Frobin, G. Leivseth, M. Biggemann, and P. Brinckmann, "Sagittal plane segmental motion of the cervical spine. A new precision measurement protocol and normal motion data of healthy adults," *Clinical Biomechanics*, vol. 17, pp. 21–31, Jan. 2002.

[13] T. Ishii, Y. Mukai, N. Hosono, H. Sakaura, R. Fujii, Y. Nakajima, S. Tamura, M. Iwasaki, H. Yoshikawa, and K. Sugamoto, "Kinematics of the Cervical Spine in Lateral Bending: In Vivo: Three-Dimensional Analysis," *Spine*, vol. 31, pp. 155–160, Jan. 2006.

[14] S.-K. Wu, L.-C. Kuo, H.-C. H. Lan, S.-W. Tsai, C.-L. Chen, and F.-C. Su, "The quantitative measurements of the intervertebral angulation and translation during cervical flexion and extension," *Eur Spine J*, vol. 16, pp. 1435–1444, Apr. 2007.

[15] S.-K. Wu, L.-C. Kuo, H.-C. H. Lan, S.-W. Tsai, and F.-C. Su, "Segmental percentage contributions of cervical spine during different motion ranges of flexion and extension," *J Spinal Disord Tech*, vol. 23, pp. 278–284, June 2010.

[16] W. Salem, C. Lenders, J. Mathieu, N. Hermanus, and P. Klein, "In vivo three-dimensional kinematics of the cervical spine during maximal axial rotation," *Manual Therapy*, vol. 18, pp. 339–344, Aug. 2013.

[17] C.-C. Lin, T.-W. Lu, T.-M. Wang, C.-Y. Hsu, S.-J. Hsu, and T.-F. Shih, "In vivo three-dimensional intervertebral kinematics of the subaxial cervical spine during seated axial rotation and lateral bending via a fluoroscopy-to-CT registration approach," *Journal of Biomechanics*, vol. 47, pp. 3310–3317, Oct. 2014.

[18] C. Zhou, H. Wang, C. Wang, T.-Y. Tsai, Y. Yu, P. Ostergaard, G. Li, and T. Cha, "Intervertebral range of motion characteristics of normal cervical spinal segments (C0-T1) during in vivo neck motions," *Journal of Biomechanics*, vol. 98, p. 109418, Jan. 2020.

[19] W. J. Anderst, E. Baillargeon, W. F. Donaldson, J. Y. Lee, and J. D. Kang, "Motion Path of the Instant Center of Rotation in the Cervical Spine During In Vivo Dynamic Flexion-Extension: Implications for Artificial Disc Design and Evaluation of Motion Quality After Arthrodesis," *Spine*, vol. 38, p. E594, May 2013.